Chapter 2

Shower Monte Carlo programs

Author: Paolo Nason

Revisors: Stefano Frixione and Roberto Tenchini

2.1 Introduction

In modern experimental particle physics, Shower Monte Carlo programs have become an indispensable tool for data analysis. From a user perspective, these programs provide an approximate but extremely detailed description of the final state in a high energy reaction involving hadrons. They provide an *exclusive* description of the reaction, as opposite to typical QCD calculations, that are only suitable to compute *inclusive* quantities.

Shower Monte Carlo programs are a mixture of several heterogeneous components, that are all needed to give a realistic description of the formation of the final state:

1. A large library of Standard Model and Beyond the Standard Model cross sections. The user can choose the hard scattering process within this library.

2. An algorithm for the generation of dominant perturbative QCD effects, called the *shower algorithm*. The shower algorithm adds to a given hard scattering a number of enhanced coloured parton emission processes. The enhancement is given by collinear and soft singularities, that can contribute large logarithms of the hard scale of the process over some typical strong interaction scale cutoff. These large log are of the order of the inverse of a

strong coupling constant, and can thus give contributions of order 1 to the hard process.

3. They implement some model of hadron formation, given the state of high energy partons that arises from steps 1 and 2.

4. They implement some model for the underlying event.

5. They include libraries for the decay of weakly unstable hadrons.

The name "Shower" is from item 2, that can be considered the kernel of a Shower Monte Carlo program. The shower generation algorithm is in essence a method for the computation of a potentially infinite number of Feynman graphs (i.e. all those that are enhanced by infrared logarithms, so that their contribution to the cross section can be considered of order one). Besides being useful for simulation of physical processes, the shower algorithms also provide a remarkably simple mental model of the most important QCD effects in high energy processes, providing insights into jet structure, fragmentation functions, structure functions and their Altarelli-Parisi evolution.

2.2 Shower basics

2.2.1 Collinear Factorization

QCD emission processes are enhanced in the collinear limit, that is to say, when an emitted parton (gluon or quark) is collinear to an incoming or outgoing parton in the scattering process. In this limit, the cross section is dominated by a subprocess in which a parent parton with small virtuality is produced that decays into the two collinear partons. There are three possible decay processes: $q \to qg$, $g \to gg$ and $g \to q\bar{q}$. The cross section factorizes into the product of a cross section for the production of the parent parton times a splitting factor. This factorization is depicted schematically in the following graphical formula, for the case of the $q \to qg$ splitting process

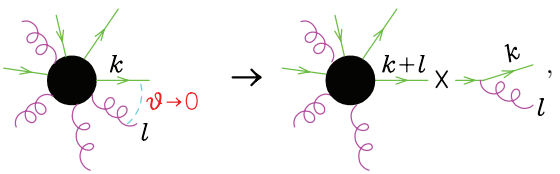

(2.1)

that has the following meaning: given a tree level amplitude with $n+1$ final state particles, assuming that a final state quark becomes collinear to a final

state gluon (i.e. their relative angle goes to zero), we have:

$$|M_{n+1}|^2 d\Phi_{n+1} \Rightarrow |M_n|^2 d\Phi_n \quad \frac{\alpha_S}{2\pi}\,\frac{dt}{t}\,P_{q,qg}(z)\,dz\,\frac{d\phi}{2\pi}. \tag{2.2}$$

where M_{n+1} and M_n are the amplitudes for the $n+1$ and n body processes, represented by the black blobs in fig. 2.1. The n and particle phase space is defined as usual

$$d\Phi_n = (2\pi)^4 \delta^4\left(\sum_{i=1}^{n} k_i - q\right) \prod_{i=1}^{n} \frac{d^3 k_i}{2k_i^0 (2\pi)^3}, \tag{2.3}$$

where q is the total incoming momentum. The parameters t, z and ϕ describe the kinematics of the splitting process: t is a parameter with the dimension of a mass, vanishing in the collinear limit, z a variable that, in the collinear limit, yields the momentum fraction of the outgoing quark relative to the momentum of the quark that has split

$$k \to z(k+l) \,\text{for}\, t \to 0, \tag{2.4}$$

and ϕ is the azimuth of the $\vec{k}, \vec{l}$ plane around to the $\overrightarrow{k+l}$ direction. $P_{q,qg}(z)$ is the Altarelli-Parisi splitting function

$$P_{q,qg}(z) = C_F\,\frac{1+z^2}{1-z}. \tag{2.5}$$

Observe that there is some arbitrariness in the definition of t and z, since dt/t is invariant if we change t by some (possibly z dependent) scale factor, and for z we only require that eq. (2.4) is satisfied in the collinear limit. We can, for example, define

$$z = \frac{k^0}{k^0 + l^0}, \tag{2.6}$$

or more generally define

$$z = \frac{k\cdot\eta}{k\cdot\eta + l\cdot\eta}, \tag{2.7}$$

that reduces to the definition (2.6) for $\eta = (1, \vec{0})$, and is perfectly acceptable as long as η does not coincide with the collinear direction. For t we can use, for example

$$\text{virtuality}: \quad t = \quad (k+l)^2 \approx E^2\theta^2 z(1-z), \tag{2.8}$$

$$\text{transverse momentum}: \quad t = \quad k_\perp^2 = l_\perp^2 \approx E^2\theta^2 z^2(1-z)^2, \tag{2.9}$$

$$\text{angular variable}: \quad t = \quad E^2\theta^2, \tag{2.10}$$

where the kinematic is illustrated in the following figure

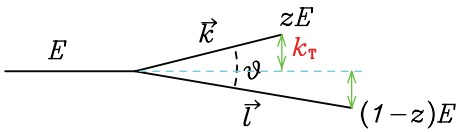

(2.11)

where $E \approx (k+l)^0$, θ is the angle between $\vec{k}$ and $\vec{l}$ and the $\approx$ relations hold for small θ. Assuming that there is nothing special about the $z \to 0$ and $z \to 1$ points, alternative choices in the definition of t and z make a difference in subleading terms in eq. (2.2), that is to say, for terms that are non-singular when $t \to 0$. Unfortunately, the $z \to 1$ and $z \to 0$ points are special: in fact, eq. (2.5) yields a divergent integration when $z \to 1$. This is an infrared divergence in QCD, since when $z \to 1$ the energy of the radiated gluon goes to zero. We will forget for the moment about this complication, and deal with collinear divergences only. The treatment of the soft region will be discussed later on.

The factorization of eq. (2.2) holds as long as the angle (or, more generally, the t variable) between the collinear partons is the smallest in the whole amplitude. This is, in some sense, natural: factorization holds if the intermediate quark with momentum $k+l$ can be considered, to all effects, as if it was on shell, that is to say, its virtuality must be negligible compared to all other energy scales entering the amplitude. It follows then that factorization can be applied recursively to an amplitude, to obtain its most singular contribution. This is shown pictorially in the following graphical formula

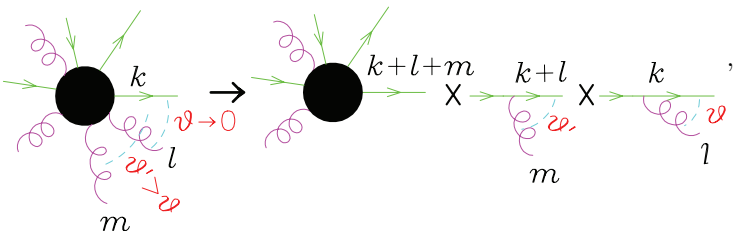

(2.12)

where we have two angles becoming small, maintaining a strong ordering relation, $\theta' \gg \theta \to 0$.

Factorization formulae, similar to the one for a qg collinear configuration (illustrated in eq. (2.1) and eq. (2.2)), also hold for the case of a gg, and $q\bar{q}$ collinear configuration, the only difference being in the form of the splitting

functions. We thus have three possibilities

$$\begin{aligned} P_{q,qg}(z) &= C_F \, \frac{1+z^2}{1-z}, \\ P_{g,gg}(z) &= C_A \left(\frac{z}{1-z} + \frac{1-z}{z} + z(1-z) \right) \\ P_{g,q\bar{q}}(z) &= t_f \left(z^2 + (1-x)^2 \right) \end{aligned} \tag{2.13}$$

Some of the $P_{i,jl}(z)$ functions are singular for $z \to 1$ or $z \to 0$. These singularities have an infrared origin. In the following, we tacitly assume that they are regularized by a tiny parameter η

$$\frac{1}{1-z} \Longrightarrow \frac{1}{1-z+\eta}, \frac{1}{z} \Longrightarrow \frac{1}{z+\eta}. \tag{2.14}$$

Notice that the $P_{i,jl}$ functions in eqs. (2.13) are related to the standard[1] Altarelli-Parisi splitting functions [1)], that are given by

$$\begin{aligned} P_{gg}(z) &= 2P_{g,gg}(z), \\ P_{qq}(z) &= P_{q,qg}(z), \\ P_{qg}(z) &= P_{q,qg}(1-z), \\ P_{gq}(z) &= P_{g,q\bar{q}}(z). \end{aligned} \tag{2.15}$$

The difference lies in the fact that the Altarelli-Parisi splitting functions tag one of the final state partons. Thus, in the $g \to gg$ case there is an extra factor of 2, because we can tag either gluons. Similarly, the $q \to qg$ splitting process is associated to two different Altarelli-Parisi splitting functions, since one can tag the final quark or the final gluon.

Strictly speaking, in the case of the $g \to gg$ and $g \to q\bar{q}$ a complication arises: an azimuthal dependent term, that has zero azimuthal average should be added to eq. (2.2). This term is a consequence of the fact that, at fixed helicities of the final state gg or $q\bar{q}$ partons, the intermediate gluon can have two helicities, and they can interfere. We will ignore this complication in the following, reminding the reader that in some shower algorithms this angular correlation effects are dealt with to some extent.

2.2.2 Fixed order calculations

The factorization formula, eq. (2.2), reminds us immediately that real radiative corrections to any inclusive quantity are divergent. This is better seen in the

[1] In fact, the unregularized Altarelli-Parisi splitting function. The difference with the standard, regularized splitting function will be clarified later.

simple example of $e^+e^- \to q\bar{q}$. The real radiative corrections to this process are given by the $e^+e^- \to q\bar{q}g$ emission process. When the gluon becomes collinear to the quark or to the antiquark, eq. (2.2) implies that there is a divergent dt/t integration. This divergence is, of course, limited by some physical cutoff, like the quark masses, or by confinement effects. But, even if we can reassure ourselves that no real infinity arises, the divergence implies that the real cross section is sensitive to low energy phenomena, that we cannot control or understand within perturbative QCD. Furthermore, the divergence yields a factor $\alpha_S(Q)\log Q/\lambda$, where Q is the annihilation scale, and λ some typical hadronic scale, that acts as a cut-off. This factor is of order 1, since $\alpha_S(Q)$ is of order $1/\log Q/\lambda$. Fortunately, one can show that, if virtual corrections are included, these divergences cancel, thanks to a mechanism known as the Kinoshita-Lee-Nauemberg theorem. In the case at hand, the order α_S virtual correction to the $e^+e^- \to q\bar{q}$ process contains a negative term behaving as $\alpha_S(Q)\log Q/\lambda$, that cancels the divergence in the real emission term. Thus, the inclusive cross section, (that, being inclusive, requires that we sum over both the $q\bar{q}$ and the $q\bar{q}g$ final states) does not depend upon the cutoff λ, and gives rise to the well-known $1 + \alpha/\pi$ correction factor to the total hadronic cross section in e^+e^- annihilation. At the same time, however, it becomes clear that it is impossible, at fixed order in QCD, to give a realistic description of the final state.

2.2.2.1 Similarities with QED

The reader familiar with the infrared problem in QED will find there some similarities with the problems discussed above. Also in QED, in order to get finite cross sections at any finite order in perturbation theory, one has to sum virtual contributions to real photon emission contributions, where photons with energy below a given resolution must be included. Thus, also in QED, at fixed order in the coupling constant, we cannot compute fully exclusive cross sections: we must always sum inclusively over soft photons below the resolution parameter.

While soft divergences are normally treated in textbooks on QED, collinear divergences are seldom considered. In fact, in electrodynamics, the mass of the electron screens the collinear divergences. This is easily understood: a massive, on shell electron cannot decay into an electron plus a photon, unless the photon has zero energy. At very high energy, however, the electron mass becomes negligible, and one should also consider the collinear singularities in QED. Charge particles, as well as photons, produced at ultra-high energy, will give rise to true electromagnetic jets. Even at more moderate energies, when considering, for example, the electron produced in the decay of a heavy object, for the purpose of mass measurements, it is better to measure the energy of the associated electromagnetic jet (as measured, for example, by an electromagnetic calorime-

ter) rather than that of the electron (as measured by a tracker), in order not to become sensitive to photon collinear emissions.

2.2.3 Exclusive final states

In order to describe the exclusive, detailed final state, we must thus sum the perturbative expansion to all orders in α_S. This is in fact possible if we limit ourselves to the most singular terms of the perturbative expansion, that is to say, all terms that carry the collinear singularities dt/t, in strongly ordered sequences of angles. Sticking to our e^+e^- example, we consider configurations where the final state q and $\bar{q}$ split into a qg ($\bar{q}g$) pair at small angle. Each final state parton is allowed to split in turn into a pair of partons with even smaller angle. Thanks to the factorization properties of the amplitude, one can easily estimate the corresponding cross section. If one allows for n splitting processes, the cross section goes as

$$\sigma_0 \alpha_S^n \int \frac{dt_1}{t_1} \dots \frac{dt_n}{t_n} \times \theta(Q^2 > t_1 > \dots > t_n > \lambda^2) = \sigma_0 \frac{1}{n!} \alpha_S^n \log^n \frac{Q^2}{\lambda^2}, \quad (2.16)$$

where Q is the annihilation energy (that provides an upper cut-off to the virtualities in the splitting processes) and λ is an infrared cut-off. The θ function here is defined to be equal to 1 if its argument is true, zero otherwise. It is because of eq. (2.16) that the collinear approximation is sometimes called leading log approximation. As discussed previously, virtual corrections to all orders in perturbation theory yield a comparable term. Their leading logarithmic contribution should then be included in order to get sensible results.

2.2.4 Counting logs

The leading logarithmic approximation requires some more explanation. Let us look at a simplified factorization formula

$$M_1 d\Phi_1 \approx M_0 \frac{dt}{t}, \quad (2.17)$$

that holds when $t \ll Q^2$, Q being the typical scales in the amplitude M_1. We have

$$\int M_1 d\Phi_1 = M_0 \int \frac{dt}{t} \theta(Q^2 > t > \lambda^2) + \mathcal{O}(1) = \log \frac{Q^2}{\lambda^2} + \mathcal{O}(1). \quad (2.18)$$

which follows from the fact that in the difference

$$\int M_1 d\Phi_1 - M_0 \int \frac{dt}{t} \quad (2.19)$$

the singularity for small t cancels. Thus the difference must be of order 1. So, even if we have said that the factorization formula holds for $t \ll Q^2$, in order to get the leading logarithm, we can integrate it for t up to Q^2. And furthermore, if we instead integrate it, for example, up to $Q^2/2$ instead of Q^2, the difference is $\log 2$, and thus is of order 1, and the leading logarithm remains the same.

2.2.5 Leading log calculation of multiparticle production

I will now just give the recipe for the calculation of our multiparticle cross section, with the inclusion of the virtual corrections at the leading log level. The outcome of the recipe is the cross section associated to each given final state. We assume that we start from some hard process, like, for example, the production of a $q\bar{q}$ pair in e^+e^- annihilation. The cross section for the hard process is computed by usual means. The recipe tells us how to compute a weight for the evolution of each coloured parton in the hard process into an arbitrary number of coloured partons.

We begin by specifying how to construct all possible event structures:

i. We choose a Born kinematics, specifying the hard interaction.

ii. For each primary coloured parton produced in the hard interaction, we consider all possible tree-level graphs that can arise from it, obtained by letting the quark split into a qg pair, the gluon split into a gg or $q\bar{q}$ pair for any quark flavour, as many times as one wishes.

iii. With each splitting vertex in the graph, one associates a t, z, and ϕ value.

iv. One imposes that the t are ordered: the t for splitting near the hard process must be less than the hard process scale Q^2, and all subsequent t's are in decreasing order as we go toward the branches of the tree-graph.

v. Given the initial hard parton momenta, and the t, z and φ variables at each splitting vertex, one reconstructs all the momenta in the tree graph.

We now specify the weight to be assigned to the given configuration:

a) The hard process has weight equal to its differential (Born level) cross section.

b) Each vertex has the weight

$$\theta(t - t_0) \quad \frac{\alpha_S(t)}{2\pi} \, \frac{dt}{t} \, P_{i,jl}(z) \, dz \, \frac{d\phi}{2\pi} \tag{2.20}$$

where $\alpha_S(t)$ is the QCD running coupling

$$\alpha_S(t) = \frac{1}{b_0 \log \frac{t}{\Lambda^2_{\rm QCD}}}. \tag{2.21}$$

In order not to reach unphysical values of the running coupling constant, we must introduce an infrared cutoff $t_0 > \Lambda^2_{\rm QCD}$. The θ function in eq. (2.20) sets the lower bound on t. The upper bound is determined by the t ordering of point (iv).

c) Each line in the graph has weight $\Delta_i(t', t'')$, where t' is the t value associated with the upstream vertex, t'' with the downstream vertex, and

$$\Delta_i(t', t'') = \exp\left[-\sum_{(jl)} \int_{t''}^{t'} \frac{dt}{t} \int_0^1 dz \quad \frac{\alpha_S(t)}{2\pi} \quad P_{i,jl}(z) \right] \tag{2.22}$$

In case the line is a final one, t'' is replaced by an infrared cutoff t_0. The weights $\Delta_i(t', t'')$ are called Sudakov form factors. They represent all the dominant virtual corrections to our tree graph.

At the end of this procedure, some hadronization model will be invoked, in order to convert the showered final state partons into hadrons. For now, in order to better clarify the shower mechanisms, we will just neglect the hadronization stage, and consider the final states (and the initial states) as made of partons.

The form of the weight at (b) is simply a consequence of a recursive application of the factorization formula. The prescription for the argument of α_S and the Sudakov form factors (c) are slightly more subtle: they arise from the inclusion of all leading-log virtual corrections to the process.

2.2.5.1 Momentum reshuffling

The final momentum assignment of step v is affected by some ambiguities, due to the fact that a parton line, when followed by a splitting process, acquires a positive virtuality larger than its mass. Because of these virtualities, the momenta of the parton must be adjusted, in order to conserve energy and momentum. For example, in the process $e^+e^- \to q\bar{q}$, the initial quarks have energy $Q/2$, and (neglecting masses) momenta equal to their energy and opposite. If the quark undergoes a splitting process, it can no longer be considered an on-shell parton, and thus its momentum must be adjusted according to the standard formulae for two body decays, including the effect of the masses of the decay products. This procedure (referred to as *momentum reshuffling*) does not affect the leading logarithmic structure of the result.

2.2.6 Typical structure of a shower

According to the recipe (i-v) and (a-c), the shower will be characterized by a tree of splittings with decreasing angles, as depicted in figure 2.1. At a given

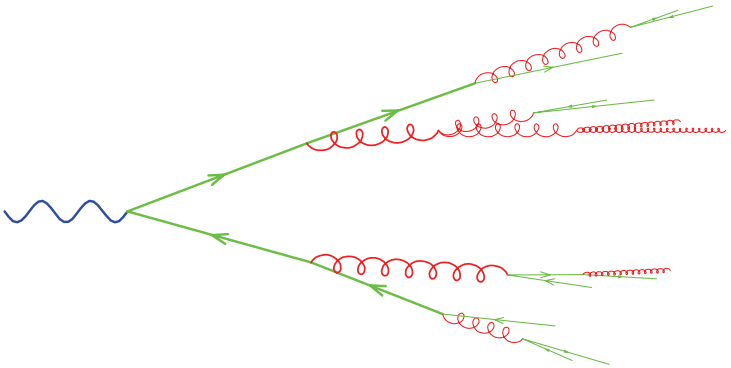

Figure 2.1: Typical shower development.

splitting vertex, the splitting angle will be typically smaller by a factor α_S than its upstream angle. As the angles become small, they will reach a point where the scale t is of the order of $\Lambda_{\rm QCD}$, so that $\alpha_S \approx 1$, angles are no longer ordered and the whole picture breaks down. At this stage the shower stops, and some model of hadronization is needed in order to complete the description of the formation of the final state. Notice also the role of the Sudakov form factors of eq. (2.22). They suppress the configurations containing lines with very large differences between upstream and downstream angles. In fact, using eq. (2.21) we estimate

$$\Delta_i(t',t'') \approx \exp\left[-C\int_{t''}^{t'}\frac{dt}{t}\quad\frac{1}{\log\frac{t}{\Lambda^2_{\rm QCD}}}\right] = \left(\frac{\log\frac{t''}{\Lambda^2_{\rm QCD}}}{\log\frac{t'}{\Lambda^2_{\rm QCD}}}\right)^C, \qquad (2.23)$$

which becomes very small if $t' \gg t''$. The behaviour of Δ as a function of t is shown in fig. 2.2. As can be seen from eq. (2.22) and from figure 2.2, the Sudakov form factor suppresses the configurations that have no radiation down to very small scales.

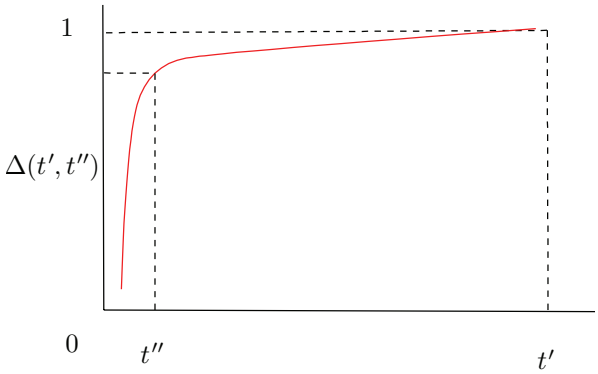

Figure 2.2: Typical behaviour of the Sudakov form factor.

2.2.7 Formal representation of a shower

In the following we will introduce some graphical notation for the representation of a shower. We use the symbol

$$\mathcal{S}_i(t, E) = \quad , \tag{2.24}$$

to represent the ensemble of all possible showers originating from parton i at a scale t. The dependence of the shower upon the parton direction is not explicitly shown, since we will not need it in the following. We can think of $\mathcal{S}_i(t, E)$ as a function defined on the set $\mathcal{F}$of all final states (by final state we mean here a set of partons with specific momentum assignments), yielding the weight of the shower for that particular final state. When writing

$$\sum_{\mathcal{F}} \mathcal{S}_i(t, E), \tag{2.25}$$

we mean sum over all final states $\mathcal{F}$, i.e. the total weight of the shower attached to parton i. Of course, $\mathcal{F}$ is not a discrete set, so, rather than a sum we should have a sum over the number and type of final state particles and an integral over their momenta. Alternatively we may imagine to divide the phase space into small cells, so that $\mathcal{F}$ can be imagined as a discrete set, and the sum notation is appropriate.

2.2.8 Shower equation

We can easily convince ourselves that the rules given in items (i-v) imply a recursive equation, that is illustrated in the following graphical equation

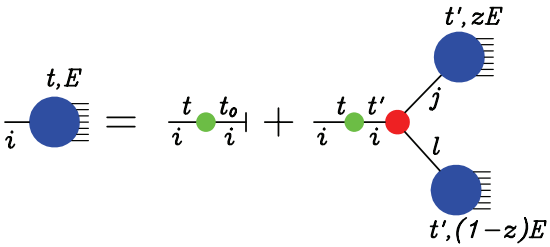

(2.26)

The meaning of the figure is quite intuitive: the ensemble of all possible shower histories is obtained by adding the case in which no branching takes place[2], to the case where one branching occurs, followed recursively by two showers starting at smaller energies and scales. The small blobs along the parton lines represent the Sudakov form factors, and the blob connecting the i, j, l partons is the splitting probability. Notice that the phase spaces of the two independent showers, after the splitting, do not overlap in our collinear approximation, because the angle at the vertex t' is larger than all subsequent angles.

The mathematical translation of eq. (2.26) is given by the equation

$$\begin{aligned}\mathcal{S}_i(t,E) \;=\; & \Delta_i(t,t_0)\mathcal{S}_i(t_0,E) + \sum_{(jl)}\int_{t_0}^{t}\frac{dt'}{t'}\int_0^1 dz\int_0^{2\pi}\frac{d\phi}{2\pi} \\ & \frac{\alpha_S(t')}{2\pi}P_{i,jl}(z)\;\;\Delta_i(t,t')\mathcal{S}_j(t',zE)\mathcal{S}_l(t',(1-z)E), \qquad (2.27)\end{aligned}$$

where the two terms correspond to the terms in the figure: no branching, plus one branching followed by two showers. $\mathcal{S}_i(t_0,E)$ represents the final state consisting of the incoming particle i alone, that has undergone no branching (since no branching is possible below t_0). Notice that the shower diagram for $\mathcal{S}_i(t_0,E)$ consist of a single line with the Sudakov form factor $\Delta_i(t_0,t_0)=1$, i.e. the shower assigns probability 1 for particle i to remain the same (i.e. to undergo no branchings).

[2]In this case the shower terminates with the given final state parton. The hadronization model will take over when all showers are terminated, building up the hadrons from the given set of coloured partons.

We can easily see that $\mathcal{S}$ satisfies the differential equation

$$t\frac{\partial \mathcal{S}_i(t,E)}{\partial t} = \sum_{(jl)} \int_0^1 dz \int_0^{2\pi} \frac{d\phi}{2\pi} \frac{\alpha_S(t)}{2\pi} P_{i,jl}(z)\, \mathcal{S}_j(t,zE)\mathcal{S}_l(t,(1-z)E) + \left[-\sum_{(jl)} \int_0^1 dz \frac{\alpha_S(t)}{2\pi} P_{i,jl}(z) \right] \mathcal{S}_i(t,E), \tag{2.28}$$

that arises because the derivative with respect to t can act on the upper limit of the integral in the second term of eq. (2.27), giving rise to the first term of eq. (2.28), or on the Sudakov form factors in both terms of eq. (2.27), giving rise to the square bracket term in eq. (2.28). Eq. (2.28) is particularly instructive. It has the following meaning: if we raise the scale of the process by an infinitesimal amount, the shower has a larger probability to split into two subshowers (the first term on the right hand side), and a smaller probability to remain the same (the second term). By summing eq. (2.28) over all possible final state, and defining

$$\mathcal{S}_i^{\rm inc}(t,E) = \sum_{\text{final states}} \mathcal{S}_i(t,E), \tag{2.29}$$

we see that $\mathcal{S}_i^{\rm inc}(t,E)$ obeys the equation

$$t\frac{\partial S_i^{\rm inc}(t,E)}{\partial t} = \sum_{(jl)} \int_0^1 dz \frac{\alpha_S(t)}{2\pi} P_{i,jl}(z) S_j^{\rm inc}(t,zE) S_l^{\rm inc}(t,(1-z)E) + \left[-\sum_{(jl)} \int_0^1 dz \frac{\alpha_S(t)}{2\pi} P_{i,jl}(z) \right] S_i^{\rm inc}(t,E). \tag{2.30}$$

We immediately see that $S_i^{\rm inc}(t,E) = 1$ satisfies the above equation, and is also consistent with the obvious initial condition $S_i^{\rm inc}(t_0,E) = 1$. We thus state the *shower unitarity* property

$$\mathcal{S}_i^{\rm inc}(t,E) = \sum_{\mathcal{F}} \mathcal{S}_i(t,E) = 1. \tag{2.31}$$

This property is at the basis of the formulation of the shower Monte Carlo algorithms. It has the following important consequence: *the total cross section computed at the Born level is equal to the total multiparticle cross section.* Of course, this statement holds in the approximation we are working with. Since we are only considering collinear-enhanced corrections, we should state more precisely that the net effect of collinear-enhanced processes is one, when we sum over all processes. We also remind the reader that this result also holds in

QED. As known from textbooks QED, large soft effects cancel in inclusive cross sections, leaving only small (i.e. $\mathcal{O}(\alpha)$) corrections to the Born cross section. The same is true also for collinear divergences, a fact that (as already remarked in 2.2.2.1) should be kept in mind when considering final stated with electrons at the LHC.

It is also instructive to check unitarity by expanding the shower order by order in α_S. At order α_S, for example, we may have at most a single splitting, since each splitting cost a factor α_S. When we sum over all final states reached by parton i, we should thus consider only the one and two parton final state. The weight of the one parton final state, at order α_S is just the Taylor expansion of the Sudakov form factor at order α_S

$$\Delta_i(Q,t_0) = 1 - \sum_{(jl)} \int_{t_0}^{Q} \frac{dt}{t} \int_0^1 dz \quad \frac{\alpha_S}{2\pi}\, P_{i,jl}(z) + \mathcal{O}(\alpha_S^2), \tag{2.32}$$

while the total weight for a two parton final state is

$$\begin{aligned} &\int_{t_0}^{Q} \frac{dt}{t} \Delta_i(Q,t) \left[\sum_{(jl)} \int_0^{2\pi} \frac{d\phi}{2\pi} \int_0^1 dz \quad \frac{\alpha_S}{2\pi}\, P_{i,jl}(z) \right] \Delta_j(t,t_0)\Delta_l(t,t_0) \\ &= \int_{t_0}^{Q} \frac{dt}{t} \sum_{(jl)} \int_0^1 dz \quad \frac{\alpha_S}{2\pi}\, P_{i,jl}(z) + \mathcal{O}(\alpha_S^2), \end{aligned} \tag{2.33}$$

that summed to eq (2.32) yields 1. At this point, one can see that the form of the Sudakov form factor is dictated by the fact that collinear singularities, according to the Kinoshita-Lee-Nauenberg theorem, must cancel.

Shower unitarity makes it possible to write the branching process as a sequence of independent branching processes (i.e. as a Markov chain). In fact, after a branching, the total weight of the two newly initiated subshowers is one, i.e. they do not influence that branching process we are considering.

2.2.9 Shower algorithm for final state showers

It is apparent now that the development of the shower can be computed numerically using a simple probabilistic algorithm. We interpret

$$\frac{\alpha_S(t')}{2\pi}\, \frac{dt'}{t'}\, P_{i,jl}(z)\, dz\, \frac{d\phi}{2\pi} \tag{2.34}$$

as the elementary branching probability in the phase space element $dt', dz, d\phi$. So

$$\frac{\alpha_S(t')}{2\pi}\, \frac{dt'}{t'} \int_0^1 dz P_{i,jl}(z) \tag{2.35}$$

is the branching probability in the dt' interval. Now we notice that, dividing the $[t, t']$ interval into N small subintervals of width δt, calling t_i the center of each subinterval, we have

$$\Delta_i(t, t') = \prod_{i=1}^{N} \left(1 - \frac{\alpha_S(t_i)}{2\pi} \frac{\delta t}{t_i} \int P_{i,jl}(z)\, dz\, \frac{d\phi}{2\pi}\right), \tag{2.36}$$

that is to say, the Sudakov form factor corresponds to the non-emission probability in the given $[t, t']$ interval. The probability that, starting at the scale t, the first branching is in the phase space element $dt', dz, d\phi$, is then

$$\Delta_i(t, t') \frac{\alpha_S(t')}{2\pi} \frac{dt'}{t'} P_{i,jl}(z)\, dz\, \frac{d\phi}{2\pi}, \tag{2.37}$$

i.e. is the product of the no-branching probability from the scale t down to t' times the branching probability in the interval $dt', dz, d\phi$. This is precisely equivalent to our shower recipe, if we remember that, because of unitarity, the total weight associated to further branchings of partons i and j is 1.

One can easily set up an algorithm for the generation of the process:

a) Generate a hard process configuration with a probability proportional to its parton level cross section (for example, for the $e^+e^- \to$ hadrons case the configuration consists of two back-to-back quarks, with energy $Q/2$, distributed as $(1 + \cos^2\theta) d\cos\theta d\phi,$). Q is in this case the typical scale of the process.

b) For each final state coloured parton, generate a shower in the following way:

   i. Set $t = Q$

   ii. Generate a random number $0 < r < 1$.

   iii. Solve the equation $r = \Delta_i(t, t')$ for t'.

   iv. If $t' < t_0$ then no further branching is generated, and the shower stops.

   v. If $t' \geqslant t_0$ then generate jl and z with a distribution proportional to $P_{i,jl}(z)$, and a value for the azimuth ϕ with uniform probability in the interval $[0, 2\pi]$. Assign energies $E_j = zE_i$ and $E_l = (1-z)E_i$ to partons j and l. The angle between their momenta is fixed by the value of t'. Given the angle and the azimuth ϕ (together with the fact that the sum of their momenta must equal to the momentum of i) the directions of j and l are fully reconstructed

   vi. For each of the branched partons j and l, set $t = t'$ and go back to step bii.

2.2.10 A very simple example

The branching algorithm in a Shower Monte Carlo resembles closely the problem of the generation of decay events from a radioactive source. We call pdt the elementary radiation probability in the time interval dt. The probability $\Delta(t')$ of having no radiation from time 0 up to time t' is given by the product of no-radiation probability in each time subinterval from 0 to t'

$$\Delta(t) = (1 - pdt)^{\frac{t'}{dt}} = \exp[-pt'] \tag{2.38}$$

and the probability distribution for the first emission is

$$\exp[-pt']pdt' = -d\Delta(t'). \tag{2.39}$$

Thus, the probability distribution for the first emission is uniform in $\Delta(t')$; in order to generate the first emission at time t', $0 < t' < t$, we generate a random number $0 < r < 1$ and solve for $r = \Delta(t')/\Delta(t)$.

2.2.11 The inclusive cross section for single hadron production

We will now compute the inclusive cross section for single hadron production, and show that it obeys the Altarelli-Parisi equation for fragmentation function. We begin by defining the fragmentation function

$$D_i^m(t,x) = \frac{1}{\delta x} \sum_{\mathcal{F}(m,x,\delta x)} \mathcal{S}_i(t,E) =$$

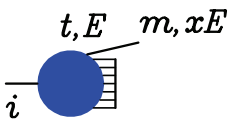

, (2.40)

where $\mathcal{F}(m,x,\delta x)$ stands here for all final states having a parton of type m with energy between xE and $(x+\delta x)E$. Notice that $D_i^m(t,x)$ does not depend upon the absolute value of the energy, since the shower recipe only involves energy fractions. It is easy to see that the fragmentation function must obey the equation represented below

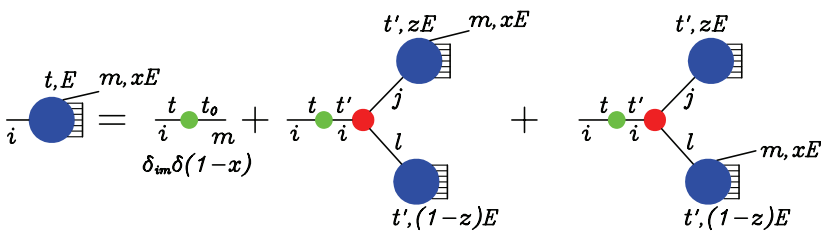

(2.41)

The meaning of the equation is quite simple. If we want to keep a final state particle of type m and energy xE, the no-radiation term can contribute only if $i = m$ and $x = 1$. In case a splitting takes place, particle m can be found in either of the two following showers. The graphical equation in eq. (2.41) can be written more precisely as follows

$$\begin{aligned} D_i^m(t,x) &= \Delta_i(t,t_0)\delta_{im}\delta(1-x) \\ &+ \sum_{(jl)} \int_{t_0}^{t} \frac{dt'}{t'} \int_x^1 \frac{dz}{z} \quad \frac{\alpha_S(t')}{2\pi} \; P_{i,jl}(z) \; \Delta_i(t,t') D_j^m(t', x/z) \\ &+ \sum_{(jl)} \int_{t_0}^{t} \frac{dt'}{t'} \int_0^{1-x} \frac{dz}{1-z} \quad \frac{\alpha_S(t')}{2\pi} \; \frac{dt'}{t'} \; P_{i,jl}(z) \; \Delta_i(t,t') D_l^m(t', x/(1-z)). \end{aligned} \tag{2.42}$$

The presence of the $1/z$ and $1/(1-z)$ on the middle member of eq. (2.42) is better understood if we imagine to multiply everything by δx; we see then that $D(t,x)$ is multiplied by δx, and $D(t', x/z)$, $D(t', x/(1-z))$ are multiplied by $\delta x/z$ and $\delta x/(1-z)$ respectively, as the definition of D suggests. As a consequence of eq. (2.28), $D_i(t,x)$ must also satisfy the equation

$$\begin{aligned} t\frac{\partial D_i(t,x)}{\partial t} &= \sum_{(jl)} \int_0^1 \quad \frac{\alpha_S(t)}{2\pi} \; P_{i,jl}(z) \; \frac{dz}{z} D_j(t, x/z) \\ &+ \sum_{(jl)} \int_0^1 \quad \frac{\alpha_S(t)}{2\pi} \; P_{i,jl}(z) \; \frac{dz}{z} \; D_l(t, x/(1-z)) \\ &+ \left[-\sum_{(jl)} \int_0^1 dz \quad \frac{\alpha_S(t)}{2\pi} \; P_{i,jl}(z) \right] D_i(t,x), \end{aligned} \tag{2.43}$$

Eq. (2.43) is just another way of writing the Altarelli-Parisi equations for fragmentation functions. Let us see in details how this works. We replace $z \to 1-z$ in the second term on the right hand side of eq. (2.43), and then use eqs. (2.15)

to combine it with the first term. We get

$$
\begin{aligned}
t\frac{\partial D_i^m(t,x)}{\partial t} &= \frac{\alpha_S(t)}{2\pi}\sum_j \int_x^1 \frac{dz}{z}\, P_{ij}(z)\;\; D_j^m(t,x/z) \\
&+ \left[-\sum_{(jl)}\int_0^1 dz\;\;\frac{\alpha_S(t)}{2\pi}\, P_{i,jl}(z)\right] D_i(t,x) \\
&= \frac{\alpha_S(t)}{2\pi}\int_0^1 dz\;\left[\frac{1}{z}\sum_j P_{ij}(z)\; D_j^m(t,x/z)\theta(z-x) - D_i^m(t,x)\sum_{(jl)} P_{i,jl}(z)\right] \\
&= \frac{\alpha_S(t)}{2\pi}\sum_j \int_x^1 \frac{dz}{z}\, \widehat{P}_{ij}(z)\; D_j^m(t',x/z). \qquad (2.44)
\end{aligned}
$$

In the last equality we have introduced the regularized Altarelli-Parisi splitting functions $\hat{P}_{ij}$. They are defined as follows

$$
\begin{aligned}
\widehat{P}_{qg}(z) &= P_{qg}(z), \\
\widehat{P}_{gq}(z) &= P_{gq}(z), \\
\widehat{P}_{qq}(z) &= P_{qq}(z) - \delta(1-z)\int_0^1 P_{q,qg}(z)dz, \\
\widehat{P}_{gg}(z) &= P_{gg}(z) - \delta(1-z)\int_0^1 \left[P_{g,gg}(z) + P_{g,q\bar{q}}(z)\right] dz. \qquad (2.45)
\end{aligned}
$$

It is easy to verify that the above definitions are equivalent to the usual regularized Altarelli-Parisi splitting functions, defined in terms of the so called "+" distributions

$$
\begin{aligned}
\widehat{P}_{gg}(z) &= 2C_A\left[\frac{z}{(1-z)_+} + \frac{1-z}{z} + z(1-z) + \left(\frac{11}{12} - \frac{n_f T_f}{3C_A}\right)\delta(1-z)\right], \\
\widehat{P}_{qq}(z) &= C_F\left[\frac{1+z^2}{(1-z)_+} + \frac{3}{2}\delta(1-z)\right], \qquad (2.46)
\end{aligned}
$$

by using the property

$$
\frac{1}{1-z+\eta} - \log\frac{1}{\eta}\delta(1-z) \Longrightarrow \frac{1}{(1-z)_+}. \qquad (2.47)
$$

2.2.12 Initial state radiation

Until now, we have considered the problem of collinear splitting affecting final state partons. The phenomenon of collinear splitting of initial state partons is

also relevant for hadronic collisions, and is commonly called *initial state radiation* (ISR from now on). The reader familiar with LEP physics will certainly remember the importance of QED ISR in e^+e^- collisions near the Z peak. QCD ISR is fully analogous, from a formal point of view, to QED ISR. There are, however, a few important differences:

- The QCD coupling is much larger: thus QCD ISR is even more important.
- The QCD coupling grows for small momentum transfer. Thus we can never neglect ISR in QCD.

Because of these differences, while for QED initial state radiation at LEP it was enough to work at one or two orders in the electromagnetic coupling, in QCD one has to resort to an all order treatment. In other words, in QCD initial state quarks and gluons *always* gives rise to an initial state showers, in the same way as final state quarks and gluons *always* manifest themselves as jets (i.e. as final state showers).

The treatment of initial state radiation in a shower Monte Carlo is very similar to the case of final state radiation. In this case, the basic factorization formula refers to the radiation from initial state particles that give rise to some hard collision. In this case, after radiation, the initial state acquires a spacelike virtuality, that is limited in magnitude by the scale of the hard process. The factorization formula, however, has essentially the same form

$$d\sigma_j^{\rm ISR}(p,\ldots) = \frac{\alpha_S}{2\pi}\frac{dt}{t}dz P_{ij}(z) d\sigma_i(zp,\ldots), \tag{2.48}$$

where now we consider a production process with a parton j entering the graph. The process is represented in the graph below

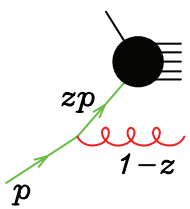

(2.49)

In this case the initial parton is on shell, and the parton with reduced momentum zp acquires a negative virtuality. This is unlike the case of final state radiation, where the virtuality is positive. Multiple initial state radiation takes place with the virtuality ordered from small (absolute) values (near the initial state parton) to large values (near the hard scattering), limited by the hardness of the scattering process. In fact, factorization holds as long as the virtuality

of the parton entering the hard scattering is negligible with respect to all the other scales entering the hard scattering amplitude. On the other hand, the radiated partons (like the gluon in (2.49)) can undergo further splitting with positive virtualities. This yields the following picture for a shower arising from an initial state parton in the collinear approximation

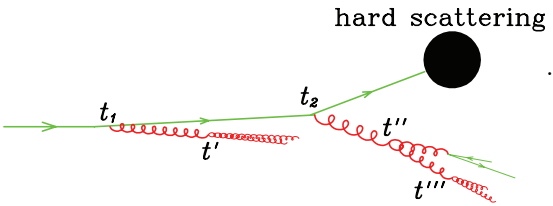

. (2.50)

We have $t_1 < t_2 < Q$, and $t_1 > t'$, $t_2 > t'' > t'''$. The intermediate lines between t_1 and t_2 and between t_2 and the hard scattering are spacelike. All other intermediate lines are timelike. The splitting functions and Sudakov form factors for initial state radiation splittings are the same that enter in the final state radiation process (differences arise only at the Next-to-Leading level). We now introduce a notation for the initial state shower

$$\mathcal{S}_i(m,x,t,E) = \quad . \tag{2.51}$$

The meaning of the notation is as follows: $\delta x \mathcal{S}_i(m,x,t,E)$ is a function on all possible states (yielding the weight of the shower for such states) having a spacelike parton of type m with energy between xE and $(x+\delta x)E$, and scale t.

The shower equation for the initial state (i.e., the spacelike shower) can be represented with the following graphical equation

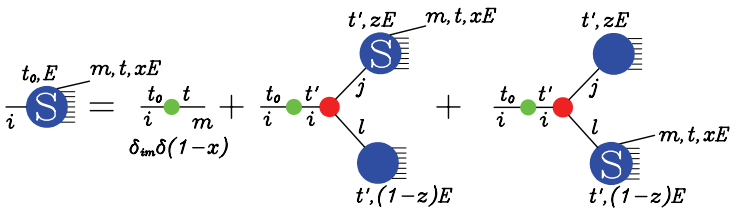

(2.52)

The blobs marked with S represent spacelike showers, while the solid blob represents the timelike showers discussed in the previous subsections. Solving

this equation would correspond to the so called forward evolution solution of the evolution equation. In modern Monte Carlo programs, it is preferred to solve the evolution equation in the opposite direction, i.e. according to the backward evolution method. The shower equation is then represented in an equivalent way, but with a recursive procedure that starts at the high scale instead of the low scale, as follows

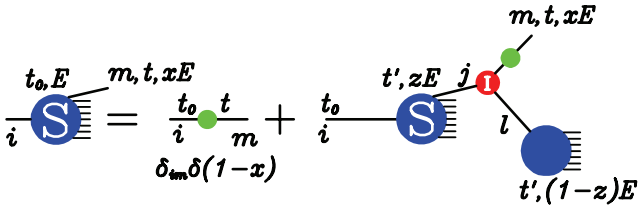

(2.53)

The blob marked with I at the splitting vertex is given by the inclusive splitting kernel P_{jm}, instead of the exclusive one $P_{j,ml}$ (this is because either branched parton can be spacelike). It is easy to convince ourselves that the pictures in fig. 2.52 and 2.53 represent the same object, with a different recursion rule.

The probability for the first branching is obtained by summing over all final states in the graphical equation of fig. 2.53. This sums yields 1 for the timelike blobs, as shown previously. Not so for the spacelike blob, that yields

$$\sum_{\mathcal{F}} \mathcal{S}_i(m, x, t, E) = f_m^{(i)}(x, t), \tag{2.54}$$

the (scale dependent) parton density function[3], and the graphical equation of fig. 2.53 yields

$$\begin{aligned} f_m^{(i)}(x,t) &= \delta_{mi}\delta(1-x)\Delta_m(t,t_0) \\ &+ \int_{t_0}^{t} \frac{dt'}{t'}\frac{dz}{z} \sum_j f_j^{(i)}(z,t') \frac{\alpha_S(t')}{2\pi} \hat{P}_{jm}\left(\frac{x}{z}\right) \Delta_m(t,t'), \end{aligned} \tag{2.55}$$

and taking the derivative of both sides with respect to t yields

$$\begin{aligned} t\frac{\partial f_m^{(i)}(x,t)}{\partial t} &= \frac{\alpha_S(t)}{2\pi} \sum_j \int_x^1 \frac{dz}{z}\, \hat{P}_{jm}(x/z)\, f_j^{(i)}(z,t) \\ &+ \left[-\sum_{(jl)} \int_0^1 dz \;\; \frac{\alpha_S(t)}{2\pi}\, P_{i,jl}(z) \right] f_m^{(i)}(x,t), \end{aligned} \tag{2.56}$$

[3]Since we are not yet considering hadrons, our parton density is now the probability to find a parton in a parton.

which is equivalent to the ordinary Altarelli-Parisi equation for the parton densities. From fig. 2.53 and eq. (2.54) we find the probability distribution for the first backward branching

$$dP_{\rm first} = \sum_j f_j^{(i)}(z,t') \frac{\alpha_S(t')}{2\pi} P_{mj}(x/z) \Delta_m(t,t') \frac{dt}{t} \frac{dz}{z} \frac{d\phi}{2\pi}. \tag{2.57}$$

In order to generate the first branching, we must express eq. (2.57) as a differential in t'. Using the Altarelli Parisi equation, from eq. (2.57) we obtain

$$\begin{aligned} \frac{dP_{\rm first}}{dt'} &= \frac{\partial f_m^{(i)}(t',x)}{\partial t} \Delta_m(t',t) + \left[\sum_{(jl)} \int_0^1 dz \ \ \frac{\alpha_S(t)}{2\pi} \, P_{i,jl}(z) \right] \times \\ & f_m^{(i)}(t',x) \Delta_m(t,t') = \frac{\partial}{\partial t'} \left[f_m^{(i)}(t',x) \Delta_m(t,t') \right]. \end{aligned} \tag{2.58}$$

Thus, the probability distribution for the first branching is uniform in $f_m^{(i)}(t',x)$ $\Delta_m(t,t')$. We just generate a random number $0 < r < 1$, and then solve the equation

$$r = \frac{f_m^{(i)}(t',x)\Delta_m(t,t')}{f_m^{(i)}(t,x)} \tag{2.59}$$

for t'. Observe that the factor $f_m^{(i)}(t,x)$ in the denominator is introduced to normalize the right hand side to 1 when $t' = t$. The Sudakov form factor $\Delta_m(t',t)$ becomes very small when t' become small. Thus, the right hand side of eq. (2.59) can become very small, its smallest value being reached when $t' = t_0$. If r is below the smallest possible value, no branching takes place. Sometimes the equivalent formula

$$\exp\left[-\sum_j \int_{t'}^t \frac{dt''}{t''} \frac{\alpha_S(t'')}{2\pi} \int_x^1 \frac{dz}{z} P_{mj}(z) \frac{f_j^{(i)}(t'',x/z)}{f_m^{(i)}(t'',x)} \right] = \frac{f_m^{(i)}(t',x)\Delta_m(t,t')}{f_m^{(i)}(t,x)} \tag{2.60}$$

is used.

We notice that, as in final state radiation, the Sudakov form factor suppresses the dt/t singularity for small values of t, thus yielding a finite expression for the first emission probability.

2.2.13 Shower algorithm for processes with incoming hadrons

We can now formulate the full recipe for the generation of a process with incoming hadrons.One can easily set up an algorithm for the generation of the process:

a) Generate a hard process configuration with a probability proportional to its parton level cross section. This cross section includes now the parton density functions evaluated at the typical scale Q of the process

b) For each final state coloured parton, generate a shower in the following way:

   i. Set $t = Q$

   ii. Generate a random number $0 < r < 1$.

   iii. Solve the equation $r = \Delta_i(t, t')$ for t'.

   iv. If $t' < t_0$ then no further branching is generated, and the shower stops.

   v. If $t' \geqslant t_0$ then generate jl and z with a distribution proportional to $P_{i,jl}(z)$, and a value for the azimuth ϕ, with uniform probability in the interval $[0, 2\pi]$. Assign energies $E_j = zE_i$ and $E_l = (1-z)E_i$ to partons j and l. The angle between their momenta is fixed by the value of t'. Given the angle and the azimuth ϕ (together with the fact that the sum of their momenta must equal to the momentum of i) the directions of j and l are fully reconstructed

   vi. For each of the branched partons j and l, set $t = t'$ and go back to step bii.

c) For each initial state coloured parton, generate a shower in the following way

   i. Set $t = Q$

   ii. Generate a random number $0 < r < 1$.

   iii. Solve the equation $r = \Delta_i(t, t')$ for t'.

$$r = \frac{f_i^{(h)}(t', x)\Delta_i(t, t')}{f_i^{(h)}(t, x)},$$

   where $f^{(h)}$ is the parton density for the hadron where parton i is found, and $x = E_i/E_h$ is the momentum fraction of the parton.

   iv. If $t' < t_0$ then no further branching is generated, and the shower stops.

   v. If $t' \geqslant t_0$ then generate j and z with a distribution proportional to $P_{ij}(z)$, and a value for the azimuth ϕ, with uniform probability in the interval $[0, 2\pi]$. Call l the radiated parton, and assign energies $E_j = zE_i$ and $E_l = (1-z)E_i$ to partons j and l. The angle between their momenta is fixed by the value of t'. Given the angle and the azimuth ϕ (together with the fact that the sum of their momenta must equal to the momentum of i) the directions of j and l are fully reconstructed

vi. For parton j, set $t = t'$ and go back to step c, cii. For parton l, set $t = t'$ and go back to step b, bii.

2.2.14 Soft divergences

Besides having collinear divergences, QCD cross sections are also affected by soft divergences, that are associated to gluons with small energy, even in the case when the angles are not small. Soft and collinear divergences can take place at the same time, giving rise to the so-called double-log singularities. In the previous discussion we have only considered collinear singularities. We have assumed that there is nothing special about the $z \to 1$ and $z \to 0$ limits in the branching, that is to say, we have reasoned under the false assumption that the splitting functions are all finite in these limits. In particular, we have neglected the kinematic constraints that arise in these regions. Let us assume, for example, that our t variable is the virtuality, and let us focus upon a single splitting at a scale t and a given value of z, that we assume to be the energy fraction. The two splitting partons have energies zE and $(1-z)E$, so they form a system with virtuality given by (neglecting their masses)

$$2z(1-z)E^2(1-\cos\theta), \tag{2.61}$$

where θ is the angle between the two partons. Thus, we must have

$$z(1-z)E^2 \geq t/4, \tag{2.62}$$

in order for the splitting to be possible. Thus, the z integration is (roughly) limited by

$$\frac{t}{4E^2} \leq z \leq 1 - \frac{t}{4E^2}. \tag{2.63}$$

If there are no soft singularities, this complication can be neglected, because, under our assumptions, $t \ll E^2$ at any stage of the branching. In fact, at the beginning of the shower $E \approx \sqrt{Q}$, and after each branching E is reduced by a factor of order 1, while $\sqrt{t}$ is reduced by a factor of order α_S. Thus the ratio $\sqrt{t}/E$ is of subleading logarithmic magnitude with respect to 1. On the other hand, since we do have soft singularities (i.e. the splitting functions are divergent for $z \to 0$ and $z \to 1$) these region of subleading logarithmic size can give contributions of order 1. Furthermore, splittings with small (or large) values of z are enhanced, and one can no longer conclude that the energy of the partons are reduced by a factor of order 1 for each branching. In other words, in order to achieve logarithmic accuracy, soft divergences should be accounted for in a proper way.

Since soft emission is associated with the production of low energy particles, we expect them to have an important impact on the multiplicity of hadrons

in the final state, and a smaller impact on the energy flow in the event. It is thus obvious that a correct treatment of soft singularities (especially in the double logarithmic region) is important in order to have a realistic description of the final state.

As discussed earlier, the choice of the hardness parameter t affects the treatment of soft divergences. Let us estimate the difference in the exponent of the Sudakov form factor when we adopt the three different definitions of the ordering parameter given in eqs. (2.8), (2.9) and eq. (2.10). If t is to be interpreted as the virtuality of the incoming line, then we must have $E^2 z(1-z) \gtrsim t$, in order for eq. (2.8) to hold[4] for some value of θ. This yields a double logarithmic integral of the form

$$\int \frac{dt}{t} \int_{t/E^2}^{1-t/E^2} \frac{dz}{1-z} \approx \frac{1}{2} \log^2 \frac{t}{E^2}, \tag{2.64}$$

the $1/(1-z)$ factor arising from the splitting functions. If instead t is interpreted as the transverse momentum, then $E^2 z^2 (1-z)^2 \gtrsim t$, and we get

$$\int \frac{dt}{t} \int_{\sqrt{t}/E}^{1-\sqrt{t}/E} \frac{dz}{1-z} \approx \frac{1}{4} \log^2 \frac{t}{E^2}. \tag{2.65}$$

If t is interpreted as the angle, we get yet another result

$$\int \frac{dt}{t} \int_0^1 \frac{dz}{1-z} \approx \log t \log \frac{E}{\Lambda}. \tag{2.66}$$

In fact, if the ordering variable is proportional to the square of the angle, the value of z is not constrained by it, and we must impose a cutoff on z in such a way that the energy of the final state particles cannot become smaller than some typical hadronic scale Λ.

It turns out that, in order to treat correctly the double logarithmic region, one should use as ordering parameter the angular variable θ. This is a profound result in perturbative QCD. It has also an intuitive explanation. Suppose that we order the emission in virtuality. Soft emissions always yield small virtuality. Thus, at the end of the shower, one has a large number of soft emissions, essentially unrestricted in angle. But soft gluons emitted at large angles from final state partons add up coherently. The soft gluons emitted from a bunch of partons with angular separation that is smaller then the soft gluon emission angle sees all the emitting partons as a single entity (see fig. 2.3). In other words it is just as if the gluon was emitted from the parton that has originated

[4]We are interested here into small values of θ, so it is fair to assume $\theta < 1$.

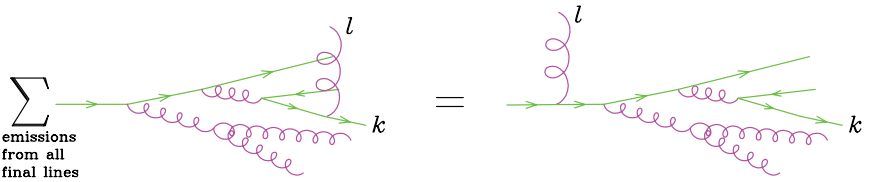

Figure 2.3: Soft emissions at large angle add coherently, i.e. they behave as if the emitter was the parton that originates the rest of the shower.

the rest of the cascade. Summarizing: if a parton is emitted at large angle, and its energy is not small, then ordering in virtuality and ordering in angle does not make any difference. If the parton energy is small, the parton should be reordered by angle. Thus, ordering in angle from the beginning gives the correct answer. Observe that angular ordering also emerges naturally in case one has jets originating from the decay of a fast moving neutral object, like, for example a relativistic Z. Angular ordering tells us that radiation at angles larger than the angle of the two primary partons in the decay of the Z should be suppressed. But this must be the case, since the radiation pattern from the Z decay should be obtainable by considering the Z decaying in its own rest frame, and then boosting all decay products with the Z velocity. The effect of the boost is precisely to squeeze all shower products towards the Z direction, with the emission at large angle from both primary partons being highly suppressed.

2.2.15 Ordering variables: HERWIG and PYTHIA

In HERWIG, the ordering variable is defined as $t = E^2\theta^2/2$, where E is the energy of the incoming parton, and θ is the angle of the two branched partons, carrying energies zE and $(1-z)E$. The Sudakov form factor is defined as follows

$$\Delta_i(t',t'') = \exp\left[-\sum_{(jl)}\int_{t''}^{t'}\frac{dt}{t}\int_0^1 dz\theta(k_T^2(t,z)-t_0)\,\frac{\alpha_S\left(k_T^2(t,z)\right)}{2\pi}\,P_{i,jl}(z)\,dz\right], \tag{2.67}$$

with $k_T^2(t,z) = tz^2(1-z)^2$. The integral in dz is always infrared divergent. An infrared cut-off is needed, and is in fact provided by the θ function, that also avoids the region where the argument of α_S becomes smaller than a given scale t_0, of the order of $\Lambda_{\rm QCD}$. If a parton of energy E branches at a scale t into two partons of energies zE and $(1-z)E$, angular ordering is achieved by choosing as the initial condition for subsequent branchings the scales t/z and $t/(1-z)$.

The PYTHIA program has never adopted the angular ordering scheme. In PYTHIA, virtualities are strictly ordered in the shower. This yields a more natural kinematics, since virtuality is kinematically ordered in a branching process. The lack of coherence, however, causes an unphysical increase in the number of soft partons, so that the particle multiplicity in e^+e^- annihilation processes does not have the correct growth with energy. The remedy in PYTHIA is to veto branchings that violate angular ordering. This scheme (virtuality ordering with angular ordering imposed by veto) yields the correct multiplicity distributions. It can be understood as follows. Configuration soft radiation at a large angle θ sum up coherently, their sum being equivalent to a soft emission from the first parent parton that comes from a branching at angles larger than θ. Thus, many emissions become equivalent to a single emission, which can be approximated to zero, as far as the multiplicity is concerned. This is what PYTHIA does. It turns out that PYTHIA, with the angular order constraint, reproduces well the energy dependence of the multiplicity. On the other hand, the author is not aware of any relevant output differences between PYTHIA and HERWIG due to the remaining differences in the treatment of soft radiation.

Recently, new showering schemes have become available. In HERWIG++, new showering variable have been introduce, that should be better from the point of view of boost invariance properties of the shower. The new versions of PYTHIA also offer an alternative showering scheme, ordered in transverse momentum, that implements a variant of the so called *dipole shower* approach, first implemented in the ARIADNE Monte Carlo.

2.2.16 Flavour, colour and hadronization.

The flavour flow in the collinear approximation is well defined. At the end of a shower we find quarks and antiquarks with a given flavour. The flavour content of the generated hadrons will depend to some extent upon the flavour content of the partons at the end of the shower, in a way that depends strictly upon the model of hadron formation.

The colour flow is not followed in the collinear approximation. In fact, the factorization formula deals with colour averaged cross sections. On the other hand, we know that final state hadrons are colour singlet. Whether or not we need to take colour into consideration depends only upon the hadronization model.

2.2.16.1 Independent fragmentation

The simplest hadronization model is the so called independent fragmentation model. This model converts each final state quark q of flavour f into hadrons.

Each final state particle is treated independently from all the others. One operates typically in the centre of mass of the parton system. One picks up a random antiflavour $\overline{f'}$, to be associated with the flavour f to form a hadron with flavour $f\overline{f'}$. The momentum of the hadron is taken to be a fraction z of the momentum of the quark q, with a probability dictated by a fragmentation function $F_{f'}(z)$, plus a transverse momentum, of the order of a typical hadronic scale, typically distributed according to a negative exponential. In order to conserve flavour and momentum, a quark with flavour f' is also generated, with momentum equal to a fraction $(1-z)$ of the initial quark momentum, and an appropriate transverse momentum. The procedure is then continued with the left-over quark, and it is stopped when the left over quark has momentum below a certain threshold. Flavour is not conserved with this procedure, unless one deals in some way with the left-over slow quarks. Also, the treatment of gluons is to some extent arbitrary. One possible approach is to always force a gluon splitting $g \to q\bar{q}$ at the end of the shower. In order to deal with baryon production, quark flavours, also diquarks are introduced. One assumes that a colour singlet baryon can be formed combining a quark and a diquark.

Independent fragmentation ignores colour, and thus does not need any colour information about the showered partons. On the other hand it has some clear drawbacks, related to the arbitrarity in the choice of the hadronization frame. Consider in fact the simple example of a virtual photon with a relatively low invariant mass, decaying into a $q\bar{q}$ pair. We assume that, because of the low mass, no parton is radiated by showering. It is clear that the multiplicity of this event, in the independent fragmentation scheme, depends upon the frame of reference in which we look at the event, the minimum multiplicity being obtained in the photon CM frame. Of course, in this case we may then decide to fragment the photon decay product in the photon rest frame, i.e. in the frame of the colour singlet system formed by the $q\bar{q}$ pair. But, in order to be consistent, every colour singlet system formed by final state partons should be decayed in its own reference frame, and this requirement is in conflict with the setup of independent fragmentation, where a quark is decayed ignoring the kinematics of all other partons.

2.2.16.2 Large N_c colour approximation

In order to deal more realistically with colour at the hadronization stage, Shower Monte Carlo's adopt the so called large N_c limit (also called planar limit), N_c being the number of colours (i.e. $N_c = 3$ in QCD). We should thus think that the number of colour is large, and keep only the dominant contribution in this sense.

The colour rules for the Feynman diagrams also become extremely simple in the large N_c limit. Colour and anticolour indices range from 1 to N_c. Each

oriented quark line is assigned a colour index and an antiquark line is assigned an anticolour index (ranging from 1 to N_c). An oriented gluon is assigned a pair of indices, corresponding to a colour and an anticolour. This gives rise to N_c^2 gluons. We know that, in fact, there are $N_c^2 - 1$ gluons, since the combination $\sum_c c\bar{c}$ (with c running over all colours) is colour neutral (i.e. is a colour singlet). However, in the limit when N_c is considered to be large, one can replace $(N_c^2 - 1) \to N_c^2$. Graphically, we may represent an oriented colour index with an arrow, and an anticolour is represented by an arrow in the opposite direction. The colour structure of a $q \to qg$, $g \to gg$ and $g \to q\bar{q}$ splitting is shown in the following figure:

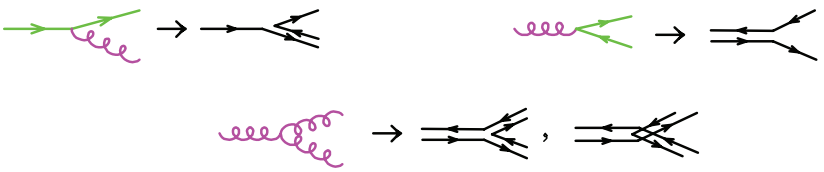

(2.68)

Notice that the two colour configurations associated to the gluon splitting vertex turn into each other by exchanging the two final state gluons.

An illustration of the large N_c limit of a contribution to the $e^+e^- \to$ hadrons cross section is given in fig. 2.4. The colour factor of the squared am-

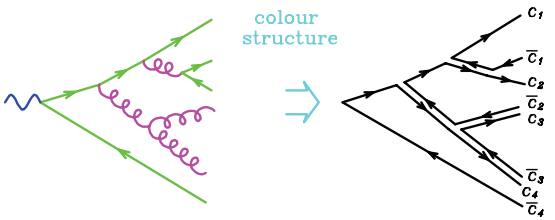

Figure 2.4: Colour structure of the square of an amplitude in the large N_c limit.

plitude is obtained by summing over the colour indices, i.e. there is a factor of N_c for each colour index. Notice that, when squaring the amplitude, interference terms are suppressed by powers of $1/N_c$. In fact, in order to have interference, two colour indices must be the same, so that one looses a factor of N_c.

When assigning a planar colour configuration to a set of showered partons, one begins by computing the Born level cross section in the large N_c limit, for each independent colour structure that is allowed, and chooses the initial

colour structure with a probability proportional to the corresponding contribution. In our $e^+e^- \to q\bar{q}$ example, there is only one such colour structure, that assigns opposite colours to the quark and the antiquark. Starting from the colour connections of the partons at the Born amplitude, one reconstructs the colour connections of all partons in the shower, according to the rules given in eq. (2.68). From the figure, we can see that there is only one way to assign colour connections in a $q \to qg$ or a $g \to q\bar{q}$ vertex. On the other hand, there are two possible assignments in the $g \to gg$ splitting, corresponding to the exchange of two final state gluons. In this case, one chooses one of the two assignments with a 50% probability. At the end of the procedure, one obtains the colour connections of all partons in the showered system.

Notice that, in the large N_c limit, it is enough to know that the quark and the antiquark are *colour connected*. One does not need to know which specific colour is assigned to them. In fact, in the limit of large N_c, the probability that two colour connected pairs of quarks have the same colour index is suppressed by a $1/N_c$ factor, and thus can be neglected.

2.2.16.3 Cluster and string based fragmentation models

The cluster and string fragmentation models are both based upon the assignments of colour connections illustrated in section 2.2.16.2.

In the cluster model, final state gluons are forced to split into quark-antiquark pairs. Then one decays each colour connected quark-antiquark pair independently. If the invariant mass of the colour connected pair is low enough, one matches mass and flavour with a corresponding hadronic two-body system (or with a resonance) with the same flavour. In angular ordered shower, one can show that configurations with colour connected pairs with large invariant mass are Sudakov suppressed (an effect known as *preconfinement*).

In the string fragmentation model, colour connected partons are collected in a system consisting of a quark, several intermediate gluons, and an antiquark. For example, in figure 2.4 there are two colour connected system, one formed by the quark with colour c_1 and the antiquark with colour $\bar{c}_1$, and the other one starting with the quark with colour c_2, including the two final state gluons with colour $[\bar{c}_2, c_3]$ and $[\bar{c}_3, c_4]$ and ending with the antiquark $\bar{c}_4$. One then imagines that a colour flux tube (i.e. a *string*) is stretched from the quark to the antiquark of the colour connected system, going through each intermediate gluon.

In the simplest case, the string is stretched between a quark and an antiquark. The hadronic system is generated by pair creation by quantum tunneling inside the string. In practice, at this stage the fragmentation algorithm is similar to the independent fragmentation case. One goes to a frame where the two string ends have opposite momenta, and, starting from each string end, one

has a fragmentation function to describe the probability to generate a hadron carrying away a given fraction of the longitudinal momentum of the string. To be more specific, let us assume that the string end has flavour f. A hadron will be generated with flavour $f\overline{f'}$, and the left over string will have a flavour f' at his end. Unlike the case of independent fragmentation, besides having a more reasonable description of the role of colour in fragmentation, also flavour is treated consistently.

In the general case, with intermediate gluons in the colour connected system, a similar procedure is adopted, with some care for the treatment of the kinks in the string associated to the intermediate gluons.

It should be made clear that fragmentation models end up being one of the most complex aspects of Shower Monte Carlo. The underlying theory (i.e. QCD) is only used as a reasonable suggestions on certain features that the models should have. The models have unavoidably a large number of parameters, that are needed in order to represent faithfully the many final state features that are observed in strong interactions.

2.2.17 Dipole approach to Shower Monte Carlo

The historical development of shower algorithms has privileged the treatment of collinear radiation. One first deals with collinear shower, and then fixes the soft radiation. A different approach has also been pursued: one generates first a soft shower, and then fixes the collinear region. In this approach one begins with a formula for soft emission from the primary partons. Unlike collinear singularities, soft singularities do not factorize in a simple way in QCD. In order to illustrate this fact we begin by first considering QED, where soft singularities do indeed factorize according to the formula

$$|M_{n+1\gamma}|^2 \Rightarrow |M_n|^2 (4\pi\alpha) \sum_{i,j=1}^{n} Q_i Q_j \frac{p_i \cdot p_j}{(p_i \cdot k)(p_j \cdot k)} \quad , \tag{2.69}$$

where p_i are the momenta of the outgoing particles, and Q_i their electric charge in positron charge units, and k is the momentum of the emitted photon. Formula (2.69) holds as long as k is much smaller than all the amplitude momenta p_i. Thus, in QED, the emission of a soft photon factorizes in terms of the original squared amplitude times the sum of so called eikonal factors, associated to photon emission from a pair of final state partons. This formula is also independent upon the spin of the emitting particles; only their electric charge counts. When $i \neq j$ each eikonal term comes from the interference of the photon emission amplitude from partons i and j, as represented graphically in fig. 2.5. In QCD, soft emission still involves the same eikonal factors that operate in QED. But the charges are replaced by colour matrices. So, while in

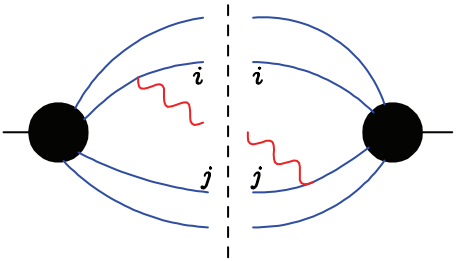

Figure 2.5: The contribution of a single eikonal factor in QED. The above figure is a common way to represent the interference of two amplitudes: the amplitude on the left, times the complex conjugate of the amplitude on the right of the dashed line.

QED the contribution of a single eikonal factor (like the one involving partons i and j in the figure) is always proportional to the Born squared matrix element, in QCD it is proportional to a square of the Born matrix elements where the colours of partons i and j have been scrambled. These colour scrambled Born contributions are potentially different among each other, so that simple, QED like factorization no longer holds. In order to recover some manageable simplicity, one takes the large N_c limits of QCD. Planar soft emissions from a planar squared amplitude always amounts to add one colour loop (i.e. to an extra factor of N_c). Thus, a planar factorization formula holds in large N_c QCD

$$|M_{n+1g}(p_1 \dots p_n, k)|^2 \Rightarrow \left[|M_n(p_1 \dots p_n)|^2 (4\pi\alpha N_c) \sum_{\text{conn.}} \frac{p_i \cdot p_j}{(p_i \cdot k)(p_j \cdot k)} \right]^{\text{Symm}}, \tag{2.70}$$

where the sum extends over all colour connected final state partons, and "Symm" stands for symmetrization in the momenta of identical particles (the planar squared amplitude not being symmetric). Thus, even in the planar limit, soft factorization is not the same as in QED. It is however easily tractable, since symmetrization is unnecessary (as long as one computes symmetric observables).

In the dipole approach, one associates Sudakov form factors to dipoles, rather than to partons, computes a no-radiation probability, and generates the emission with a procedure similar to the one used in the single parton shower approach. One generates a t for each dipole, and then picks the hardest t to decide which dipole is emitting. In the limit when the emitted gluon is parallel

to a final state parton, one adjusts the eikonal factors in such a way that they become correct even if the energy of the emitted parton is not small, in order to reproduce the Altarelli Parisi splitting probability. If the emitting parton is a gluon, two dipoles can contribute to its emission, and this has to be accounted for properly.

2.3 Underlying event

The hadronization model deals with final state partons, turning them into hadrons. Also initial state partons require some treatment, in order to give a realistic description of the physics of the hadronic remnants. First of all, what we have introduced as the parton density to find a parton in a parton (eq. (2.54)) should be immediately interpreted as the probability to find a parton in the incoming hadron. In the forward evolution scheme, this would require to introduce an initial parton density at the scale t_0. In the backward evolution scheme this is unnecessary: one compute the cross section with the full pdf at the scale of the process, using standard pdf parametrization. However, when the backward shower stops (i.e. a scale $t < t_0$ is generated in the backward evolution formalism), we should provide some model for the structure of the remaining part of the incoming hadron. This is a subtle problem, that cannot be treated in a rigorous way in QCD. The crudest approach one can think of, is to force initial state gluons at the end of the shower to arise from a quark in backward evolution, then let the remaining diquark in the incoming proton, carrying the left over momentum of the initial hadron, hadronize with the remaining particles in the event. In other approaches, if the backward shower stops with a gluon, the remaining quarks in the incoming hadron are put into a colour octet state, and this system is broken up with various rules, to yield objects that the hadronization mechanism can handle. There is some evidence 5 that, in order to represent the activity of the underlying event in a reasonable way, the effect of multiparton interactions must also be included. In other words, one must assume that the remnants of the incoming hadrons can undergo relatively hard collisions. Even this phenomenon is implemented with phenomenological models in Shower Monte Carlo programs. Among the ingredients entering these models, one assumes that partons have a given transverse distribution in a hadron. The cross section for secondary interactions is assumed to be given by the partonic cross section with an appropriate cutoff in transverse momentum. This cutoff has to be carefully tuned, since the partonic cross section diverges as the cutoff goes to zero. The momentum of the spectator partons has to be properly rescaled, to account for the momentum taken away by the parton that initiates the spacelike shower. Flavour and colour of the spectators has to be properly adjusted.

2.4 Shower Monte Carlo resources

Here I collect useful references to Shower Monte Carlo physics. First of all, the pedagogic introductions in refs. [7], [3] and [5] offer an alternative introduction to the one presented here.

In ref. [2] a primer on the main available Monte Carlo codes and methods is given.

The PYTHIA manual [6] is a valuable source of information on several aspects of Shower Monte Carlo physics. In the original HERWIG paper [4], more thorough discussion of the problem of soft radiation can be found.

In the web page `http://www.hepforge.org/`, links to various Monte Carlo programs, as well as to tools typically used in this framework (like jet algorithms and the like) can be found.

References

1 . Guido Altarelli and G. Parisi. Asymptotic freedom in parton language. *Nucl. Phys.*, B126:298, 1977.

2 . M. A. Dobbs et al. Les houches guidebook to monte carlo generators for hadron collider physics. 2004.

3 . R. Keith Ellis, W. James Stirling, and B. R. Webber. Qcd and collider physics. *Camb. Monogr. Part. Phys. Nucl. Phys. Cosmol.*, 8:1–435, 1996.

4 . G. Marchesini et al. Herwig: A monte carlo event generator for simulating hadron emission reactions with interfering gluons. version 5.1 - april 1991. *Comput. Phys. Commun.*, 67:465–508, 1992.

5 . Torbjorn Sjostrand. Monte carlo generators. 2006.

6 . Torbjorn Sjostrand, Stephen Mrenna, and Peter Skands. Pythia 6.4 physics and manual. *JHEP*, 05:026, 2006.

7 . B. R. Webber. Monte carlo simulation of hard hadronic processes. *Ann. Rev. Nucl. Part. Sci.*, 36:253–286, 1986.